

Pore Structure and Thermal Conductivity of Cryogenic Concrete

Reginald B. Kogbara*, Srinath R. Iyengar, and Eyad A. Masad

Mechanical Engineering Program, Texas A&M University at Qatar, P.O. 23874, Education City, Doha, Qatar.

Email: regkogbara@cantab.net

Syeda Rahman, Zachary C. Grasley, and Dan G. Zollinger

Zachry Department of Civil Engineering, Texas A&M University, College Station, TX 77843, USA

Abstract—The pore structure, which controls the main properties of concrete, evolves due to phase changes in the pore network during cryogenic freezing of concrete. This study investigates the influence of such pore structure evolution on the thermal conductivity of different concrete mixtures. Such information would be useful in the design of low thermally conductive concrete for use in liquefied natural gas (LNG) containment structures. Five concrete mixtures including hardened cement paste were prepared using different aggregates and admixtures. The mixtures incorporated river sand as fine aggregate, and traprock and limestone as coarse aggregates. Mixtures without aggregates incorporated different amounts of blast furnace slag (BFS) and granulated polyurethane foam (PUF) and sawdust. The porosity and pore size distribution of concrete specimens were monitored at ambient and freezing temperatures using proton nuclear magnetic resonance (NMR). Thermocouples inserted into concrete specimens at different radial locations monitored the temperature history during cryogenic freezing and thawing. A new inverse analysis technique that simultaneously fits the temperature profile at two different locations during thawing of frozen specimens was used for thermal conductivity determination. The results indicate that among the different mixtures, the total porosity shows a stronger correlation ($R^2 = 0.88$) with thermal conductivity than the mean pore size ($R^2 = 0.52$) at freezing temperatures. The total porosity ($R^2 = 0.75$) was also more influential at ambient temperature. The thermal conductivity results so far suggest the possibility of designing a low thermally conductive concrete by improving on concrete mixture designs incorporating some of the aforementioned admixtures.

Index Terms—LNG containment structures, nuclear magnetic resonance, pore size distribution, porosity, thermal conductivity

I. INTRODUCTION

Knowledge of the thermal properties of concrete is important in evaluating the thermal effects that arise in concrete structures exposed to variable thermal fields. Containment tanks for liquefied natural gas (LNG) are subjected to large temperature swings during cooling to cryogenic temperatures (i.e. ≤ -165 °C). The development of the ACI 376-11 standard [1] may increase the impetus

for tank designs utilizing concrete for primary LNG containment [2, 3]. Current construction methodology for LNG containment tanks utilizes a primary tank, constructed from welded 9% Ni steel that contains the LNG under normal operation. The primary tank is enclosed within a secondary concrete tank that is designed to contain an LNG spill from the primary containment and resist the associated increased vapor pressure that develops in the event of an accidental leak or spill from the primary containment [4]. An expanded perlite insulation between the primary and secondary tank walls acts as a barrier to limit the inflow of heat and the associated boil-off of the stored LNG. This involves a large volume of insulation foam, which is quite expensive [4-6]. Therefore, for an all-concrete containment tank, the development of low thermally conductive concrete is important, as it would reduce insulation costs and the large volume of foam glass insulation waste generated onsite with a conventional tank [5].

The development of low thermally conductive concrete for LNG containment structures requires knowledge of the thermal conductivity during cryogenic freezing. However, standardized test methods for evaluating the heat transfer properties of concrete are, in general, not feasible at cryogenic temperatures. Previous efforts in this direction utilized a mathematical solution that presumes linearity of the thermal constitutive functions [7, 8]. However, it is expected that the thermal behavior of cryogenic concrete is highly non-linear owing to the changing internal composition (i.e., pore water progressively freezing). The primary source of expected non-linearity is the evolving microstructure associated with phase changes (ice, water, and vapor) in the pore network. Moreover, point sources or sinks of heat due to the heat of fusion of water were not accounted for in previous studies. Thus, a new method for measuring the heat transfer properties of concrete at cryogenic temperatures is required. Furthermore, changes in pore structure can be monitored by proton nuclear magnetic resonance (^1H NMR) as the decay of proton (from water molecules) magnetization varies with different pore sizes. Thus, NMR relaxation times can provide information on the pore size distribution. The total porosity can also be obtained through comparison of the NMR signal of a

Manuscript received May 20, 2018; revised November 28, 2018.

concrete core with that of an equivalent amount of water [9].

In light of the above, this study sought to investigate the pore structure evolution (due to cryogenic freezing) of different concrete mixtures evaluated for direct LNG containment using NMR. There is a dearth of information on the influence of the evolving microstructure on the thermal conductivity of cryogenic concrete. Hence, it was also the objective of the study to investigate the effect of pore structure evolution on thermal conductivity of the concrete mixtures. This entails development of a new inverse analysis technique for thermal conductivity determination that does not involve implicit assumptions about linearity of the constitutive laws. The resulting information from this study would be useful in the design of low thermally conductive concrete for use in LNG containment structures.

II. METHODOLOGY

A. Production of Concrete Mixtures

Five concrete mixtures including hardened cement paste were prepared using different aggregates and admixtures as detailed in Table 1. Two mixtures previously found to be suitable for direct LNG containment incorporated river sand as fine aggregate, and traprock and limestone as coarse aggregates [2, 3, 10]. The maximum aggregate size used was 19 mm.

Two other mixtures without conventional aggregates were targeted for low thermal conductivity. These incorporated different amounts of blast furnace slag (BFS, a supplementary cementitious material) and low thermal conductivity materials such as polyurethane foam (PUF) and sawdust granulated (< 0.475 mm) using a commercially available blender. The properties of these materials have been documented elsewhere [10-12]. Type I Portland cement was used for casting all specimens. The exact dimensions of the specimens used were 75 mm diameter by 150 mm long cylinders for the thermal conductivity tests and 38 mm diameter by 50 mm cores for the NMR tests. The specimens were cured under water and tested after 28 days curing age.

B. Cryogenic Cooling and Thawing of Concrete Specimens

The concrete cylinders and cores were placed in a temperature chamber (Cincinnati Sub Zero, Ohio, USA) in a moist condition and cooled from ambient (20 °C) to cryogenic temperatures. (≤ -165 °C) through liquid nitrogen injection in 50 minutes. The default (highest) cooling capacity of the temperature chamber was employed to encourage pore structure changes via microcracking in the concrete mixtures. Type T thermocouples connected to data loggers (*Supco*, New Jersey, USA) were employed to record the temperature history of the concrete specimens. The thermocouples were inserted into predrilled holes of about 75 mm depth at the center and mid-radial location, and also placed on the surface of the concrete specimens. The cooling function of the temperature chamber was turned off after

the temperatures of all concrete specimens were ≤ -165 °C. Thereafter, the specimens were carefully taken out of the chamber with the aid of cryogenic personal protective equipment. Specimens for thermal conductivity determination were then placed in an environment maintained at 20 °C to warm to ambient temperature. While cores for NMR testing were all stored in a Corafoam® thermal insulation material (i.e., rigid polyisocyanurate foams, *Duna Corradini*, Modena, Italy) until tested.

C. NMR Testing

NMR measurements were performed with a 2 MHz rock core analyzer using a 54 mm probe (*Magritek*, New Zealand). The NMR technique has been detailed in a previous related publication [4]. The measurements were performed on the same core for a given concrete mixture on three occasions, namely, before cryogenic freezing, while in the frozen state, and after thawing and re-saturation. Temperature measurements of the frozen cores preserved in insulation material showed that, on average, the temperatures ranged from -70 °C to 0 °C during the NMR testing. The T_2 relaxation data of a water-saturated core was measured using the Carr-Purcell-Meiboom-Gill (CPMG) sequence with 100 μ s echo time, an inter-experimental delay time of 6,500 ms and 100 - 200 scans. The CPMG decay was analyzed with a Lawson and Hanson non-negative least square fit method using Prospa software (*Magritek*, New Zealand). The software then outputs the logarithmic mean T_2 (a proxy for the mean pore size) in the command line history field.

D. Thermal Conductivity Determination

The thermal conductivity of the concrete mixtures at ambient temperature was determined using a KD2 thermal properties analyzer (*Decagon Devices*, Inc., Washington, USA) with 60 mm probe length. The device provides direct readings of the thermal conductivity. A new inverse analysis technique was employed for thermal conductivity determination during cryogenic freezing. The heat transfer equation for a one-dimensional cylindrical coordinate system neglects the point heat source due to freezing or melting of pore water, and can be written as:

$$\frac{1}{r} \frac{\partial}{\partial r} \left(k(T) r \frac{\partial}{\partial r} T(r,t) \right) = \rho C(T) \frac{d}{dt} T(r,t). \quad (1)$$

where ρ is density, $C(T)$ is the specific heat capacity at constant stress, $T(r,t)$ is temperature as a function of radial location, r , and time, t ; $k(T)$ is the thermal conductivity, ∂ is the partial derivative, and $\frac{d}{dt}$ is the material time derivative.

The inverse analysis technique solves (1) for the initial and boundary conditions specific to the experimental setup. Estimated temperature history is then fitted with the measured temperature history. Values of $k(T)$ and $C(T)$ are continuously changed until the curves coincide with each other completely with negligible error. The

approach is simplified by assuming quadratic functional forms for these two parameters such that:

$$k(T) = k_0 + k_1 T(r,t) + k_2 T^2(r,t), \quad (2)$$

$$\text{and } C(T) = C_0 + C_1 T(r,t) + C_2 T^2(r,t). \quad (3)$$

where k_0 , k_1 , k_2 , C_0 , C_1 , and C_2 are coefficients.

The Mathematica software (Version 10, Wolfram Research, USA) command, *NDSolve*, is used to solve the nonlinear heat transfer equation (1) and the *Manipulate* command is used to manipulate the internal variable in (2) and (3).

The temperature history at two different radial locations is simultaneously fitted to calculate the internal coefficients in (2) and (3) (see Fig. 1). A unique set of thermal conductivity and specific heat as a function of temperature can then be obtained as the cylinder is thawed from cryogenic to ambient temperatures. The algorithm was used to determine the thermal conductivity of the concrete mixtures within 6 temperature ranges (-165 to -120 °C, -120 to -90 °C, -90 to -60 °C, -60 to -20 °C, -20 to 0 °C and 0 to 20 °C) critical to pore structure changes in cryogenic concrete [2, 3]. The analysis of the

specific heat capacity of the concrete mixtures is beyond the scope of this paper.

III. RESULTS AND DISCUSSION

A. NMR and Thermal Conductivity Measurements before Cryogenic Freezing

The T_2 distribution - a proxy for the pore size distribution - is shown alongside the cumulative porosities of the different concrete mixtures before cryogenic freezing in Fig. 2a and 2b, respectively. While the relationships between the thermal conductivity (determined using KD2 thermal properties analyzer) and the logarithmic mean T_2 (proxy for mean pore size) and cumulative porosity are shown in Fig. 2c and 2d, respectively. In the T_2 distribution in Fig. 2a, the peaks denote pores of different sizes, while the pore volume is denoted by the amplitude of the peaks. The gel and capillary pores are represented by the first and second peaks, respectively, which are present in all concrete mixtures. Subsequent peaks denote larger (or very large) pores and cracks.

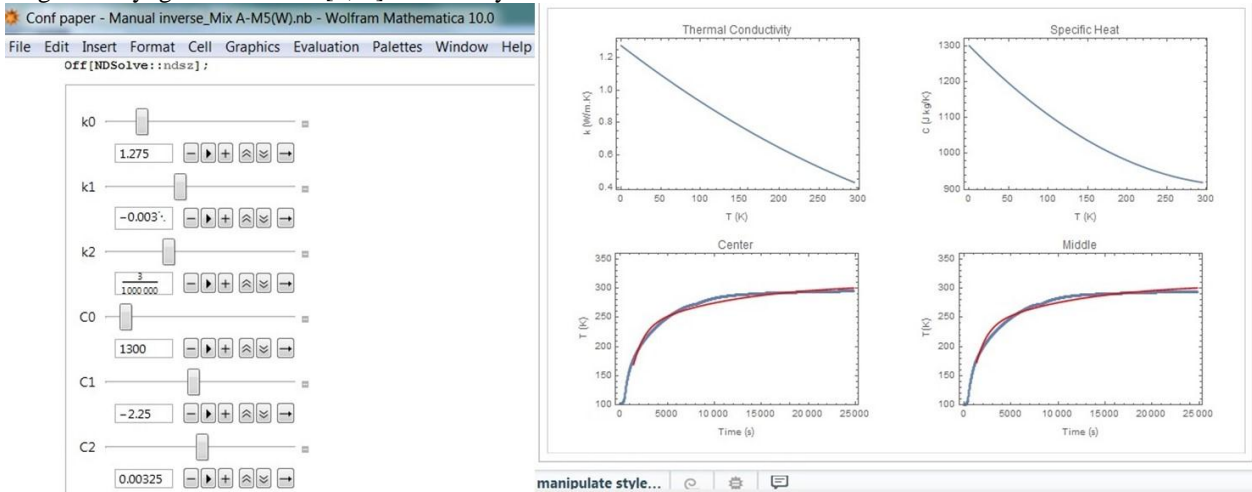
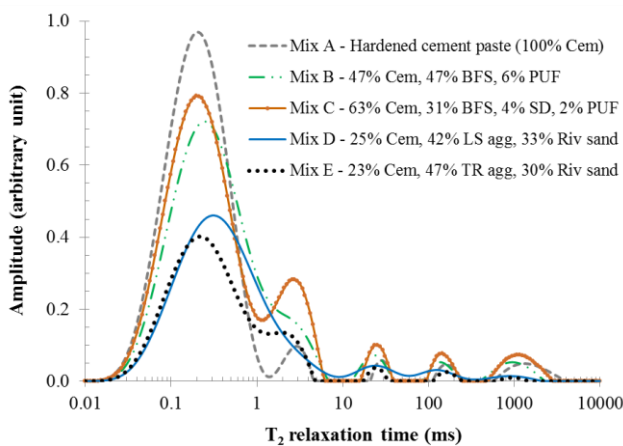
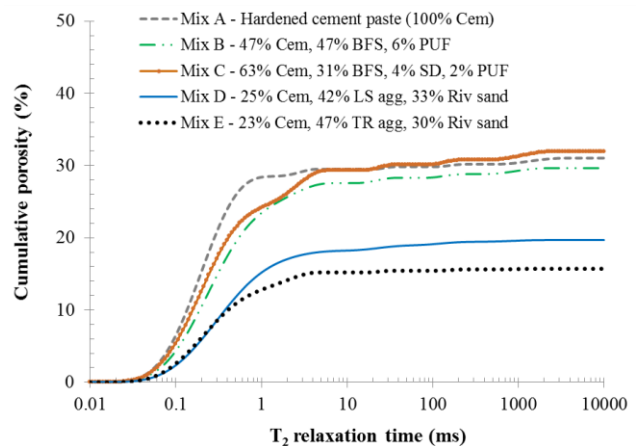


Figure 1. Example screenshot from Mathematica software showing thermal conductivity and specific heat determination in which the temperature history at different radial locations is simultaneously fitted to calculate the internal coefficients in (2) and (3) using the *Manipulate* command.



(a)



(b)

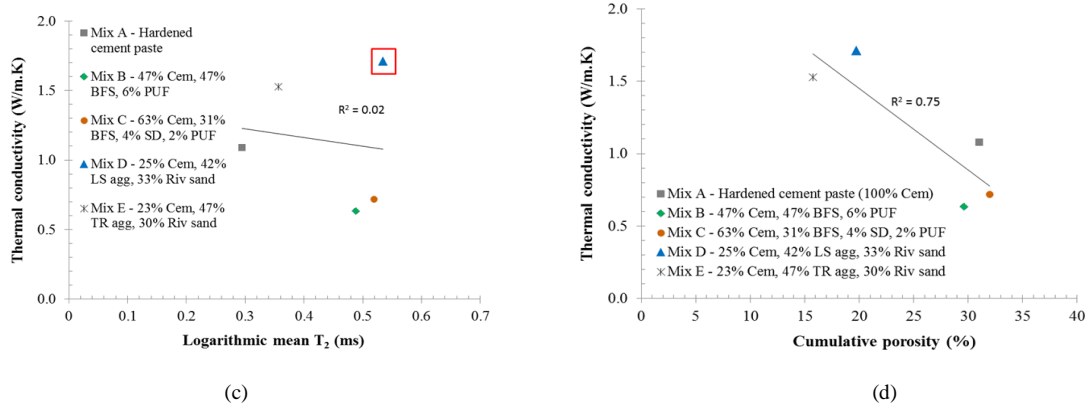


Figure 2. (a) T_2 distribution, (b) cumulative porosity, (c) thermal-conductivity-log mean T_2 relationship, and (d) thermal-conductivity-porosity relationship of the concrete mixtures before cryogenic cooling. Note: Cem – cement, BFS – blast furnace slag, PUF – polyurethane foam, SD – sawdust, LS – limestone, agg – aggregate, Riv – river, TR – traprock, T_2 distribution and log mean T_2 are proxies for pore size distribution and mean pore size, respectively.

Fig. 2a shows that the gel pores increase with an increase in the cement content of the concrete mixture. This is probably because the calcium silicate hydrate (CSH) gel can only be produced in the originally water-filled capillary cavities in fresh cement paste [13]. The mixtures without aggregates (Mixes A – C) had much higher porosities than both mixtures with aggregates (Mixes D and E), while the presence of sawdust in Mix C led to the highest cumulative porosity (Fig. 2b). The relationship in Fig. 2c and 2d suggest that, among the different concrete mixtures, at ambient temperature the total porosity ($R^2 = 0.75$) is more influential rather than the mean pore size ($R^2 = 0.02$). However, R^2 for the mean

pore size changes to 0.55 if the limestone mixture (marked by a red square) is excluded (Fig. 2c). Hence, this needs to be confirmed for a range of mixtures with widely different porosities.

B. NMR Measurements after Cryogenic Freezing

Fig. 3 shows the T_2 distribution and cumulative porosities of the concrete mixtures after cryogenic freezing. The NMR measurements made on the frozen cores that were preserved in insulation material over the $-70\text{ }^\circ\text{C}$ to $0\text{ }^\circ\text{C}$ range are shown in Fig. 3a and 3b. While NMR measurements on thawed and re-saturated cores are shown in Fig. 3c and 3d.

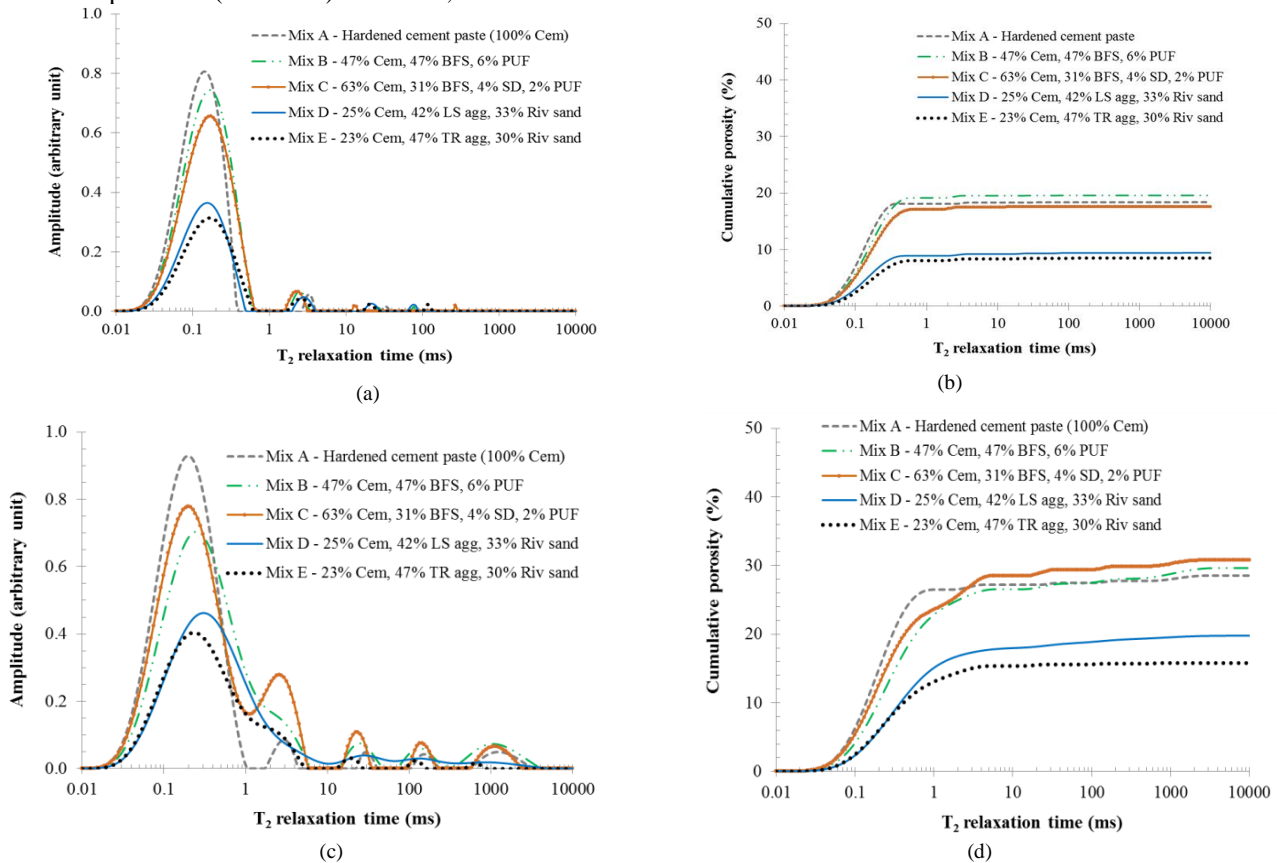


Figure 3. Pore structure of the concrete mixtures after cryogenic cooling, during thawing (approx. $-70\text{ }^\circ\text{C}$ to $0\text{ }^\circ\text{C}$) in terms of (a) T_2 distribution, and (b) cumulative porosity, and after re-saturation in terms of (c) T_2 distribution, and (d) cumulative porosity. Note: Cem – cement, BFS – blast furnace slag, PUF – polyurethane foam, SD – sawdust, LS – limestone, agg – aggregate, Riv – river, TR – traprock, T_2 distribution is a proxy for pore size distribution.

Comparison of Fig. 2b and 3b indicate that about 40 – 50% of the total pore space is blocked by ice during the thawing process. The measurements also show that within the aforementioned temperature range, most of the larger or very large pores are filled with ice, while only about 20% of the gel porosity is blocked by thawing ice. In contrast, on average, about 70% of the capillary porosity of the concrete mixtures is blocked by thawing ice. Mixes B and C with higher volumes of larger (or very large) pores show the most shifts in total porosity trend after cryogenic freezing within the -70 °C to 0 °C range. The porosities of both mixtures were initially lower/higher and then subsequently higher/lower than that of hardened cement paste (see Fig. 2b and 3b). There were no noticeable changes in the porosities after thawing and re-saturation, except for Mixes A and C with the highest initial porosities, whose total porosities decreased by 1 – 2%. Both mixes had the highest cement contents and hence gel pore volume, and the gel pores indicated much of the porosity reduction. It was recently documented that for hardened cement paste samples stored at high relative humidity, some non-freezable water in the CSH gel is not readily regained on rewetting. This is attributed to the formation of calcium bridges between silicate groups via the loss of some of the initial water ligands and their replacement by oxygen ligands bound to the silicate groups [14].

C. Thermal Conductivity - Pore Structure Relationship after Cryogenic Freezing

The thermal conductivity of the different concrete mixtures over the six temperatures ranges considered is shown in Fig. 4. While Fig. 5 shows the relationships between thermal conductivity and pore structure in the -70 °C to 0 °C temperature range after cryogenic freezing (during thawing). The thermal conductivity demonstrates a decreasing trend with increasing temperatures (Fig. 4) as documented in the literature [6]. The thermal conductivity values of the concretes determined by the

new technique is also within the documented range [6]. The most porous concrete mixtures generally showed the lowest thermal conductivities. Among the different mixtures, the total porosity shows a stronger correlation ($R^2 = 0.88$) with thermal conductivity than the mean pore size ($R^2 = 0.52$) (Fig. 5a and 5b) similar to the behavior at ambient temperature. Although, the mean pore size shows a much higher correlation with thermal conductivity at freezing temperatures than at ambient temperature (compare Fig. 2c and 5a). The increase in thermal conductivity with increasing mean pore size at freezing temperatures (Fig. 5a) is probably due to the presence of more ice (with higher thermal conductivity) in the larger pores [6]. Especially, as most of the ice resides in such pores as shown by the NMR measurements in Fig. 3.

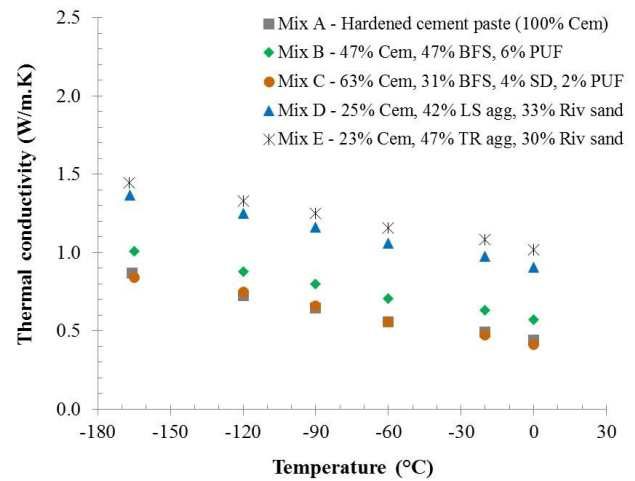


Figure 4. Thermal conductivity of the concrete mixtures during warming to ambient temperature. Note: Cem – cement, BFS – blast furnace slag, PUF – polyurethane foam, SD – sawdust, LS – limestone, agg – aggregate, Riv – river, TR – traprock. Thermal conductivity values were determined for 6 temperature ranges (-165 to -120 °C, -120 to -90 °C, -90 to -60 °C, -60 to -20 °C, -20 to 0 °C and 0 to 20 °C) for cryogenically frozen concrete specimens placed in an environment maintained at 20 °C.

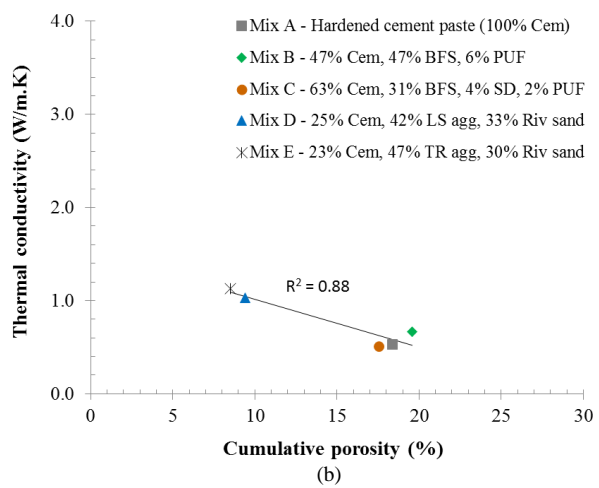
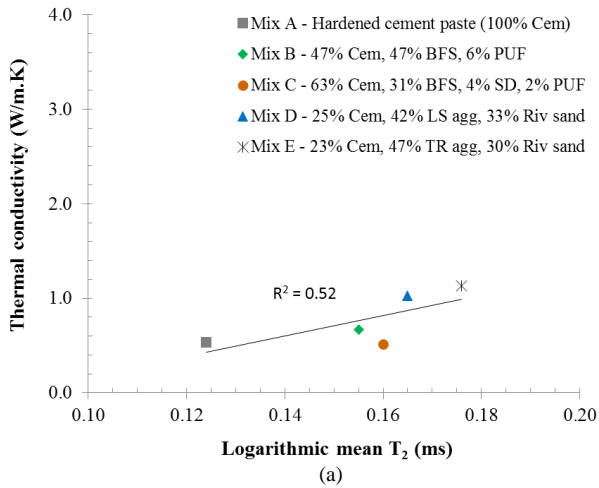


Figure 5. Relationship between pore structure and thermal conductivity of frozen concrete specimens during thawing, in terms of (a) logarithmic mean T_2 , and (b) cumulative porosity. Note: The thermal conductivity values were determined for the temperature range, -70 to 0 °C, during thawing to be consistent with the average temperature range during NMR testing of the frozen cores.

Furthermore, Mix C showed thermal conductivity values relatively lower than the other mixtures (but

similar to hardened cement paste) at cryogenic temperatures, as well as the lowest value when cooled to

ambient temperature (Fig. 4). It also had a compressive strength greater than the minimum (28 MPa) specified in the ACI 376-11 code (Table 1). Hence, with improved

mixture design, a low thermally conductive concrete that incorporates some of its constituents can be developed.

TABLE I. MIXTURE DESIGN AND PROPERTIES OF THE CONCRETE MIXTURES

Concrete mixture	Cement	Trap rock	Limestone	River sand	BFS	PUF	Saw dust	Water	w/cm ratio	Bulk density	28-d compressive strength
(kg/m ³)											(MPa)
Mix A	1769	-	-	-	-	-	-	525	0.30	2195	40
Mix B	560	-	-	-	560	77	-	390	0.35	1545	7
Mix C	858	-	-	-	430	20	57	490	0.38	1535	33
Mix D	512	-	868	694	-	-	-	215	0.42	2425	36
Mix E	512	1056	-	670	-	-	-	215	0.42	2650	40

Note: BFS – blast furnace slag, PUF - polyurethane foam, w/cm – water/cementitious-material.

IV. CONCLUSIONS

The influence of pore structure evolution due to cryogenic freezing on the thermal conductivity of different concrete mixtures has been investigated. These were done using NMR and a new inverse analysis technique for thermal conductivity determination under cryogenic conditions. The results indicate that among the different mixtures, the total porosity shows a stronger correlation ($R^2 = 0.88$) with thermal conductivity than the mean pore size ($R^2 = 0.52$) at freezing temperatures. The total porosity ($R^2 = 0.75$) was also more influential at ambient temperature. The thermal conductivity results so far suggest the possibility of designing a low thermally conductive concrete for use in LNG containment structures. This can be achieved with improved concrete mixture designs incorporating some of the admixtures used here. For example, improving upon Mix C with thermal conductivity of 0.4 – 0.8 W/mK in the ambient to cryogenic temperature range. Future studies may consider the effect of mineralogical and chemical composition on pore structure evolution in cryogenic concrete.

ACKNOWLEDGEMENTS

This publication was made possible by the NPRP award (NPRP9-448-2-176: Constitutive modelling and investigation of bond-slip relationship in concrete for direct liquefied natural gas containment) from the Qatar National Research Fund (a member of the Qatar Foundation). The statements made herein are solely the responsibility of the authors.

REFERENCES

[1]. ACI 2011 ACI 376 - Code requirements for design and construction of concrete structures for the containment of refrigerated liquefied gases and commentary. An ACI Standard. (Farmington Hills, MI: American Concrete Institute).

[2]. R. B. Kogbara, S. R. Iyengar, Z. C. Grasley, E. A. Masad, and D. G. Zollinger, "Non-destructive evaluation of concrete mixtures for direct LNG containment," *Mater. Des.*, vol. 82, pp. 260-272, Oct. 2015.

[3]. R. B. Kogbara, S. R. Iyengar, Z. C. Grasley, S. Rahman, E. A. Masad, and D. G. Zollinger, "Correlation between thermal deformation and microcracking in concrete during cryogenic cooling," *NDT & E Int.*, vol. 77, pp. 1-10, Jan. 2016.

[4]. K. Hjortset, M. Wernli, M. W. LaNier, K. A. Hoyle, and W. H. Oliver, "Development of large-scale precast, prestressed concrete liquefied natural gas storage tanks," *PCI J.*, vol. 58, pp. 40-54, Fall 2013.

[5]. K. Hoyle, S. Oliver, N. Tsai, K. Hjortset, M. LaNier, and M. Wernli, "Composite concrete cryogenic tank (C3T): A precast concrete alternative for LNG storage," presented at the 17th International Conference & Exhibition on Liquefied Natural Gas, Houston, TX, April 16-19, 2013.

[6]. N. Krstulovic-Opara, "Liquefied natural gas storage: Material behavior of concrete at cryogenic temperatures," *ACI Mater. J.*, vol. 104, pp. 297-306, May-June 2007.

[7]. A. E. Lentz, and G. E. Monfore, "Thermal conductivity of concrete at very low temperatures," *J. PCA R&D Labs*, vol. 7, pp. 39-46, 1965.

[8]. M. Yoshiwa and A. Iwata, "Performance characteristics of an apparatus based on the curve-fitting method for measuring thermal properties at cryogenic temperatures," *Cryogenics*, vol. 17, pp. 273-282, 1977.

[9]. L. R. Stingaciu, L. Weiermüller, S. Haber-Pohlmeier, S. Stapf, H. Vereecken, and A. Pohlmeier, "Determination of pore size distribution and hydraulic properties using nuclear magnetic resonance relaxometry: A comparative study of laboratory methods," *Water Resour. Res.*, vol. 46, W11510.

[10]. R. B. Kogbara, S. R. Iyengar, Z. C. Grasley, S. Rahman, E. A. Masad, and D. G. Zollinger, "Relating damage evolution of concrete cooled to cryogenic temperatures to permeability," *Cryogenics*, vol. 64, pp. 21-28, Nov.-Dec. 2014.

[11]. R. B. Kogbara, A. Al-Tabbaa, and J. A. Stegemann, "Comparisons of operating envelopes for contaminated soil stabilised/solidified with different cementitious binders," *Environ. Sci. Pollut. Res.*, vol. 21, pp. 3395-3414, 2014.

[12]. N. J. Al-Thani, J. Bhadra, D. Abdulmalik, I. Al-Qaradawi, A. Alashraf, and N. K. Madi, "Positron annihilation study on polyaniline nanocomposite used for Pb (II) ion removal," *Desalin. Water Treat.*, vol. 57, pp. 27374-27385, 2016.

[13]. K.K. Aligizaki, *Pore Structure of Cement-based Materials: Testing, Interpretation and Requirements*, 1st ed. London, UK: CRC Press, 2006, ch. 1, pp. 5-7.

[14]. E. Gartner, I. Maruyama, and J. Chen, "A new model for the CSH phase formed during the hydration of portland cements," *Cem. Concr. Res.* vol. 97, pp. 95-106, July 2017.